Dynamics of 3D Real Foam Coarsening

C. Monnereau and M. Vignes-Adler*
Laboratoire des Phénomènes de Transport dans les Mélanges du CNRS
4ter, Route des Gardes F-92190 Meudon, France
(Received 29 October 1997)

Dynamics of a polydisperse 3D dry foam was experimentally investigated by means of a novel nondestructive method, more precisely by optical tomography associated to a foam reconstruction algorithm. The foam coarsening law obeys to a 3D extension of the classical von Neumann coarsening law of 2D foams. It is obtained as $\langle V_f\rangle^{-1/3} d\langle V_f\rangle/dt = k'(f - \langle f\rangle)$. $\langle V_f\rangle$ is the mean volume of f-faced bubbles, k' a diffusion constant equal to the single film gas diffusion coefficient, and $\langle f\rangle$ is the mean number of faces per bubble. [S0031-9007(98)06375-3]

PACS numbers: 82.70.Rr

Until now, many studies have been devoted to the morphology of two dimensional foams, which are much simpler and easier to visualize than the three dimensional ones. The way the 2D foam structure evolves is now well known [1]. The film network reorganizes during time because of gas diffusion from a small bubble towards a bigger neighbor due to the difference of Laplace pressure (coarsening) or because of film ruptures (coalescence). It also evolves because of morphological rearrangements such as a topological change ($T1$) where two neighboring bubbles generate a new face or such as a transformation ($T2$) where a bubble disappears. von Neumann has demonstrated that the law of coarsening in 2D foams for a bubble depends only on its topology (its number of edges, n) and not on its area:

$$\frac{dA_n}{dt} = \kappa(n - 6), \tag{1}$$

with A_n the area of the n edges bubble and κ a diffusion constant. 6 is the mean value of edges per bubble in a 2D foam with an infinite number of bubbles. Thus, a n-edges bubble has a constant area, shrinks, or grows with time, if $n = 6$, $n < 6$, or $n > 6$, respectively. Experimentally, relation (1) holds on the average [2].

Now, in a dry 3D foam, the bubbles are polyhedral and the structure is therefore much more complex and difficult to observe. The foam structure is such that the liquid films organize themselves to minimize their surface at a given gas volume. From the area-minimizing principle, Plateau derived the first laws of foam geometry: (i) the edges (Plateau borders) are formed by three liquid films, with mutual angles equal to 120°; (ii) the vertices are formed by four edges with mutual angles equal to 109.5° [the tetrahedral angle, $\cos^{-1}(-1/3)$]. Moreover, each liquid film has a constant curvature, because the pressure difference between the two sides of a film is inversely proportional to its mean curvature (Laplace's law).

By studying photographs, Matzke found that the average number of faces per bubble $\langle f\rangle = 11.00$ for 400 bubbles belonging to the first three layers and $\langle f\rangle = 13.7$ for the 600 internal bubbles [3]. Foam coarsening was investigated by Glazier *et al.* by magnetic resonance imaging [4] and by Durian *et al.* by multiple light scattering [5]. Glazier *et al.* proposed for 3D cellular structures numerically generated by a Potts model, the following normalized law of coarsening by analogy with (1):

$$V_f^{-1/3}\frac{dV_f}{dt} = k(f - f_0), \tag{2}$$

where k is a diffusion coefficient and f_0 was not found equal to $\langle f\rangle$ but to 15.8 [2,6]. In [7], Weaire and Glazier deduced empirically that

$$f_0 = \langle f\rangle\left(1 + \frac{\mu_2}{\langle f\rangle^2}\right). \tag{3}$$

where $\mu_2 = \langle f^2\rangle - \langle f\rangle^2$ is the foam disorder.

As far as we know, the foam structure and its dynamics have never been simultaneously studied independently. It is the purpose of this paper to fill this gap by numerizing real foam structures and performing measurements on the elements of individual bubbles. Hence, optical tomography associated to a foam reconstruction algorithm was developed as a nondestructive method to investigate the morphology, topology, and dynamics of a 3D foam, i.e., the time evolution of the structure, the bubble volumes, and the area of 3D transparent dry foams [8]. The present paper is focused only on dynamics.

Experimental.—The foam cell consists of a cylindrical container (5 cm diameter and 10 cm height) covered by a glass lid, whose lower part is a sintered glass plate. Its bottom is connected to a liquid reservoir by a flexible Teflon tube in order to control the capillary pressure P_γ in the foam by changing the height level (Δh) between the container and the reservoir. Both container and reservoir are fixed to the same motorized table (z) in order to keep Δh constant during scanning. In the whole experiment, Δh is fixed to 60 mm, i.e., $P_\gamma = 595$ Pa. Thus, the Plateau border curvatures are kept nearly constant along the foam column and during the coarsening experiment.

In order to prevent contamination by antifoaming materials, great care was taken in cleaning the cell [8]. A polydisperse foam with a mean diameter bubble size of

 0031-9007/98/80(23)/5228(4)$15.00

5 ± 2 mm was then generated in the cylindrical container by blowing filtered U-nitrogen through a pro-Pasteur pipette directly into an aqueous solution of SDS (0.1% wt) and dodecanol (0.003% wt) at a flow rate around 55 $\mathrm{mm^3\,s^{-1}}$. Its density ρ, surface tension γ, and dynamic shear viscosity μ are 1.01 $\mathrm{g\,cm^{-3}}$, 40.0 $\mathrm{mN\,m^{-1}}$, and 0.99 cP, respectively. The films of SDS and dodecanol in these proportions immediately evolve into black films which are rigid and extremely stable in time [9].

The cell was lit with a cold and polarized illumination plate. Optical tomography consisted of scanning the foam by means of a Lhesa CCD camera equipped with a very thin depth-of-field (1 mm thick) Micro-Nikkor 105 mm $f/2.8$ objective and connected to a graphic digitization card. The camera was focused on the center of the upper surface of the foam to analyze only the central bubbles without any contact with the lateral walls of the cell (Fig. 1). During scanning, the optical system was kept fixed while the foam cell was displaced in the focus plane, by steps $\Delta z = 1$ mm. Images of the slices were digitized and stored in a microcomputer. A whole scanning took 45 sec for 28 slices. Since nitrogen has a low solubility in water, the foam coarsening was negligible during scanning. Foam coarsening was followed during 9 h. Besides, in an *ad hoc* cell, the film thickness h_{film} and the nitrogen diffusion coefficient D_{film} in the film formed by one attached bubble to the free surface of the same aqueous solution were measured by videomicrointerferometry [10]. It was found that $h_{\mathrm{film}} = 35$ nm and $D_{\mathrm{film}} = 3.7 \times 10^{-5}$ $\mathrm{mm^2\,s^{-1}}$ [8].

Reconstruction.—Only the central core of the foam was processed. The liquid films are transparent (common black films) and only the Plateau borders network (edges) appears in the images (Fig. 1). The principle of foam reconstruction is to determine the locations of all the foam vertices from a series of such images of foam slices, and to numerically reconstruct the minimal surfaces connecting the vertices in the same arrangement as the real foam. The physical assumption underlying the reconstruction procedure is that capillarity and gravity are acting on the foam structure. The *equilibrium* structure is therefore obtained when the total energy of the foam is minimum. Both gas and liquid are treated as incompressible.

In the individual images, there are sharp parts which belong to the actual focus plane $z = \mathrm{const}$, and fuzzy zones which do not belong to it. The sharp points correspond to the bubbles vertices. Mousse software (Mousse is a foam analyzer software from Noesis Inc., Surface Evolver compatible) analyzes by a morphological gradient method the whole series of images to find in which one each vertex has the best sharpness; this determines the z vertex coordinate. Then, in the image to which the vertex belongs, segments corresponding to the edges are detected by means of a Hough transformation and their intersection precisely gives the x and y coordinates of the vertex. Each vertex is numbered. The spatial resolution is 30 μm in the x and y directions, and the accuracy of the measurement is 0.5 mm in the z direction, which corresponds to half the distance between two successive images.

The foam reconstruction procedure involves three main steps:

(i) Determination of the equivalent polyhedral structure having the same number and arrangement of bubbles, faces, edges, and vertices. It consists of defining, orientating, and naming each edge, each face, and each bubble of the foam, knowing that the faces are oriented with their normal going out. At this stage, the structure of the 3D foam is a set of polyhedra with straight edges which does not satisfy the Plateau laws (Fig. 2).

(ii) Calculation of the total energy E (total surface energy E_s + gravitational energy E_p) of the equivalent polyhedral structure. E_p is neglected because the liquid volume is negligible in dry foams. The foam films solely contribute to E_s; the film energy per unit area is taken as 2γ. Actually, the disjoining pressure contribution to the

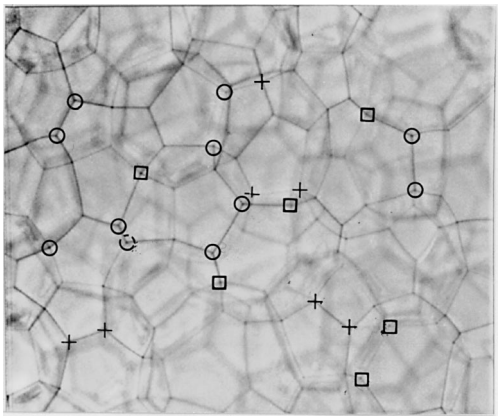

FIG. 1. Image of a slice in the central parallelpipedic core (2.2×1.6 $\mathrm{cm^2}$). This slice is located at the center of the cylindrical foam column whose internal diameter is $\phi = 5$ cm; vertices belonging to image $i - 1$ (□); i (○), and $i + 1$ (+).

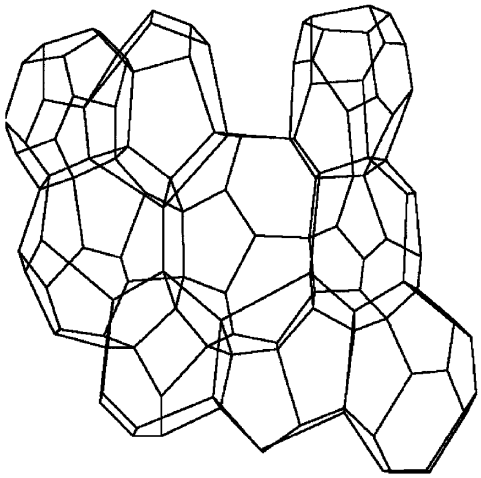

FIG. 2. Projection of the structure of the first bubble layer.

film energy can be neglected since only common black films (≈35 nm) are obtained here. Therefore, for this foam sample

$$E \cong E_s = 2\gamma \times A_{\text{film}}, \tag{4}$$

where A_{film} is the total film area.

(iii) Minimization of E with Surface Evolver software (Surface Evolver is a minimization software developed by Brakke [11]) under the constraint that the bubble volumes are constant and for the following boundary conditions: (i) on boundary bubbles, the edges that appear with 2 reconstructed faces instead of 3, and the vertices with 3 reconstructed edges instead of 4 are fixed; (ii) the vertices, edges, and faces in contact with the porous plate are allowed to move only in the plate plane. The 3D foam structure is displayed by Geomview software (Geomview is a graphic display software [11]). The bubble faces are triangulated [Fig. 3(a)] and A_{film} is minimized by moving the facet vertices by a gradient descent method until convergence [11]. This makes the faces and edges more curved and the polyhedral angles closer to the tetrahedral angle. The reconstructed foam is the one with a minimal value of A_{film} [Fig. 3(b)]. On the reconstructed foam, the bubble, faces, edges, and vertices are analyzed, and the geometrical properties measured.

Foam dynamics.—The foam has been reconstructed at $t = 0$, 1, 3, 6, and 9 h after its creation. It consists of 5 layers of bubbles among which 48 entire bubbles are reconstructed, which corresponds to 412 faces, 800 edges, and 437 vertices.

Two types of bubbles should be distinguished: the external bubbles that belong to the top layer or to the bottom layer in contact with the porous plate (20 bubbles), and the internal bubbles that belong to the others layers (layers 2, 3, and 4: 28 bubbles).

It is crucial to notice that the present discussion is focused only on internal bubbles belonging to the central core which are at least 3 bubbles far from the lateral walls of the cell (Fig. 1). Most of the faces are pentagonal with the mean number of edges per face $\langle n \rangle_{\text{int}} = 5.11$ and it was found that $\langle f \rangle_{\text{int}} = 13.39 \pm 0.05$ which is in good agreement with the literature values [3,12,13]. We have checked that the fluctuations around $\langle f \rangle$ became lower than ± 0.05 as soon as more than 20 bubbles taken at random are considered to calculate $\langle f \rangle$. Neither Kelvin nor Weaire-Phelan structures were found in this foam although they are theoretically the most stable structures in monodisperse foams [12]. The foam disorder μ_2 was found equal to 1.8. Another independent experiment gave $\langle f \rangle = 13.75 \pm 0.05$ for 57 internal bubbles with $\mu_2 = 0.85$.

Each bubble was followed individually. The mean volume $\langle V(t) \rangle_{\text{int}}$ was constant during time $\langle V(t) \rangle_{\text{int}} = 58 \pm 1$ mm^3. The foam was not in a scaling state, where $\langle V(t) \rangle \propto t^{\alpha}$, with $\alpha = 1.5$ measured by Durian [5]. Polydispersity was lower at the beginning (smaller standard deviation, STD = 14 mm^3), and it increased with time (STD = 17 mm^3). No topological transformation was observed, i.e., a f-faced bubble keeps f faces during the whole experiment. Hence, the observed volume variations are not due to topological transformation, but to coarsening.

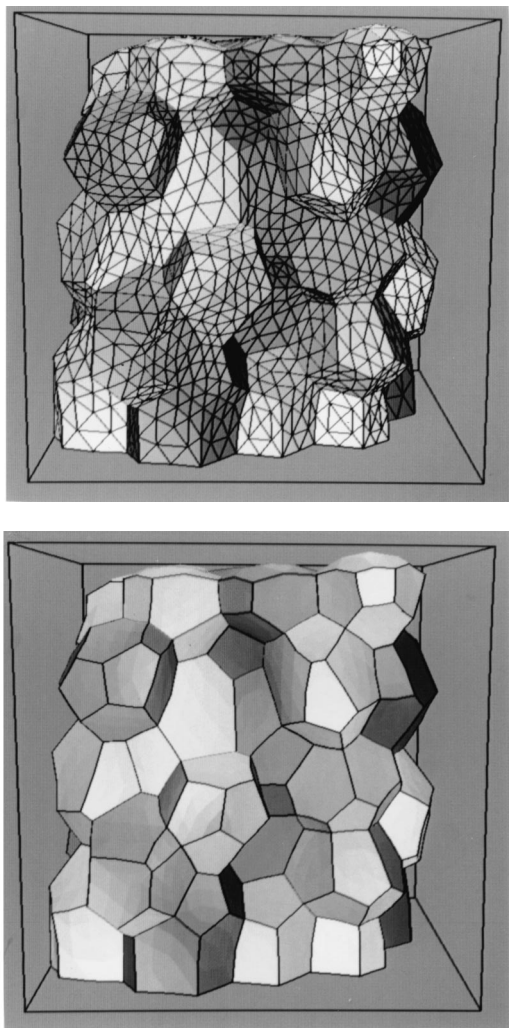

FIG. 3. Foam reconstruction at 9 h: (a) with triangulation; (b) without triangulation.

Equation (2) holds on average [7]. In a polydisperse foam generated at random as the present one, a bubble has on the average 13 larger or smaller neighbor bubbles which also evolve because of their own 13 larger or smaller neighbors either by shrinking or by expanding. This confers collective properties to the foam. Hence, it is not possible here to calculate a slope with an acceptable regression coefficient for each internal bubble assuming that Eq. (2) is verified. Introduction of the mean volume of the f-faces internal bubbles $\langle V_f(t) \rangle$ instead of $V_f(t)$ into Eq. (2) yields

$$\langle V_f(t) \rangle^{-1/3} \frac{d\langle V_f(t) \rangle}{dt} = k'(f - f_0), \tag{5}$$

where k' is a diffusion coefficient.

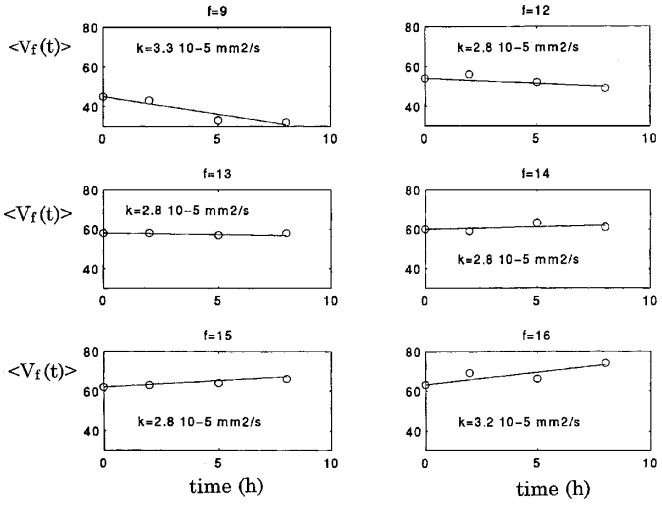

FIG. 4. $\langle V_t(t)\rangle$ for internal bubbles. The regression coefficients are reported in physical units. The lines are the fits.

Integration of (5) *at constant topology* between t_0 and t yields

$$\langle V_f(t)\rangle^{2/3} = \frac{2}{3}\, k'(f - f_0)\,(t - t_0) + \langle V_f(t_0)\rangle^{2/3}. \quad (6)$$

$\langle V_f(t)\rangle$ are plotted versus time for $f = 9$–16 in Figs. 4. In the average, bubbles with a larger number of faces have larger volumes. Some tendency to $\langle V_f(t)\rangle$ equalization occurred at the beginning as in 2D foams [1]. Then coarsening became much more regular. The time origin has therefore been shifted to $t_0 = 1$ h.

The sign of the slope changes between $f = 13$ and $f = 14$. k' was calculated for each f by a mean square method. It is an f-independent constant, since $k' = 2.8 \times 10^{-5}\ \mathrm{mm^2\,s^{-1}}$ except for $f = 9$ and $f = 16$ for which $k' = 3.3 \times 10^{-5}\ \mathrm{mm^2\,s^{-1}}$ (Figs. 4). It is almost equal to the diffusion coefficient $D_{\mathrm{film}} = 3.7 \times 10^{-5}\ \mathrm{mm^2\,s^{-1}}$ that was measured independently on a single film.

The best fit of Eq. (6) was found for $f_0 = 13.4$; it should be emphasized that this value is exactly the mean number of faces per bubble $\langle f\rangle$ which was measured on the present foam, as in von Neumann's law (1). f_0 calculated using Eq. (3) equals 13.5. Hence, this experimental result compares well with the numerical one of [6]. The foam disorder is here low and the above correction is negligible.

In conclusion, the dynamics of coarsening of a slightly disordered foam with rigid films is likely given by Eq. (5) where $f_0 = \langle f\rangle$. A bubble with less than $\langle f\rangle$ faces should shrink and a bubble with more than $\langle f\rangle$ faces should expand. As far as we know, this work is the first experimental investigation of a 3D analog of von Neumann's law.

We are indebted to Dr. B. Prunet-Foch for his advice in implementing the optical tomography. The partial financial support from the Centre National des Etudes Spatiales is greatly acknowledged.

*Author to whom correspondence should be addressed.

[1] D. Weaire and N. Rivier, Contemp. Phys. **25**, 59 (1984).
[2] C. Sire, Phys. Rev. Lett. **72**, 420 (1994).
[3] E. Matzke, Am. J. Botany **33**, 58 (1946).
[4] J. A. Glazier, B. Prause, C. P. Gonatas, J. S. Leigh, and A. M. Yodh, Phys. Rev. Lett. **75**, 573 (1995).
[5] D. J. Durian, D. A. Weitz, and D. J. Pine, Science **252**, 686 (1991).
[6] J. A. Glazier, Phys. Rev. Lett. **70**, 2170 (1993).
[7] D. Weaire and J. A. Glazier, Philos. Mag. Lett. **68**, 6 (1993); **68**, 363 (1993).
[8] C. Monnereau, Ph.D. dissertation, Université de Marne-la-Vallée, Champs-sur-Marne, France 1998.
[9] K. J. Mysels, K. Shinoda, and S. Frankel, *Soap Films* (Pergamon, New York, 1957).
[10] H. M. Princen and S. G. Mason, J. Colloid Sci. **20**, 353 (1965).
[11] K. Brakke, Exp. Math. **1**, 2 (1992); **1**, 141 (1992).
[12] R. Phelan, D. Weaire, and K. Brakke, Exp. Math. **4**, 181 (1995).
[13] T. Aste, D. Boosé, and N. Rivier, Phys. Rev. E **53**, 6181 (1996).